

# Detecting forgery in image time series based on anomaly detection

N I Evdokimova<sup>1</sup> and V V Myasnikov<sup>1,2</sup>

<sup>1</sup>Samara National Research University, Moskovskoe shosse 34, Samara, Russia, 443086

<sup>2</sup>Image Processing Systems Institute - Branch of the Federal Scientific Research Centre "Crystallography and Photonics" of Russian Academy of Sciences, Molodogvardeyskaya str. 151, Samara, Russia, 443001

**Abstract.** Increasing complexity of image forgery methods is an actual problem nowadays. This problem rises due to the expansion of fields that use digital images in their work. Image time series show the dynamics of the scene and allow it to be compared over time. This paper proposes a new algorithm for detecting forgeries of the single digital image in an image time series described a scene. This algorithm uses analysis of errors set that were computed during reconstruction of the analyzed image using other images of series. The first part of the paper describes the proposed algorithm consisted of three stages. The second part of the paper describes forgery detection using morphological image filtering based on guided contrasting. The third part of the paper contains comparison of considered algorithms and investigation results of intra-image copy-move and inter-image copy-move detection.

## 1. Introduction

Image time series describe dynamic of an scene. Analysis of an image time series lets modeling an image that can be next in the image time series. Also, it allows deciding authenticity of the image. There are several approaches to image forgery detection. These approaches may use unique artifacts left by the camera, unique artifacts arising after compression and, finally, temporal and spatial correlations [1]. Methods that used temporal and spatial correlation can divide into two categories. Techniques from the first category based on analysis of images pixel data [5], [6], [7] whereas methods from the second category use object level of images [8].

Forgeries may be created to add a new object to the scene or to hide any existing. Image time series forgery detection has its distinctive features compared to image matching. Every image of an image time series is obtained at different moments of time. Two adjacent images of an image time series can be captured under different conditions of illumination, weather or seasonal conditions. In this paper, the algorithm invariant to the conditions for obtaining images of the series is proposed.

The proposed algorithm uses a correlation between corresponding fragments of neighboring images in the series. In this paper, the concept of anomaly applies for image series forgery detection. In the global sense, an anomaly is a fragment of data that does not correspond to the precisely defined concept of normal behavior [2]. In the sense of this paper, all fragments that are marked as anomaly are considered forgeries.

This work consists of three parts. In the first part, an algorithm for image time series forgery detection based on the anomalies detection are presented. An algorithm of forgery detection using morphological image filtering based on guided contrasting [3] is given in the second part. The third part contains the comparison of both algorithms presented in the first part and the second part.

## 2. Forgery detection based on the anomalies detection

Let there is an image time series  $I_t(n_1, n_2)$ ,  $t$  - image number in time series ( $t = \overline{0, T}$ ,  $T \geq 1$ ). Every image has the same size  $N_1 \times N_2$  ( $n_1 \in [0, N_1]$ ,  $n_2 \in [0, N_2]$ ) and captures the same scene at different moments of time.

For definiteness, it is assumed that the image  $I_0(n_1, n_2)$  is checked for forgeries although it may be located in the image time series anywhere. The fragments  $I_t(m_1, m_2)$  of all images are analyzed in the sliding window  $D(n_1, n_2) \subseteq \overline{0, N_1 - 1} \times \overline{0, N_2 - 1}$ ,  $(m_1, m_2) \in D(n_1, n_2)$ .

### 2.1. Image fragment description

The fragments  $I_t(m_1, m_2)$  are described in  $k$  steps,  $k = 2^p$ ,  $p > 2$ .

On the  $k = 1$  step, the fragment  $I_0(m_1, m_2)$  is reconstructed by linear combination of corresponding fragments  $I_1(m_1, m_2), \dots, I_T(m_1, m_2)$  for all possible positions of sliding window  $D$ :

$$I_0(m_1, m_2) \approx \sum_{t=1}^T \alpha_t I_t(m_1, m_2) \quad (1)$$

using mean squared deviation  $\varepsilon_1^2$  minimization:

$$\varepsilon_1^2 = \frac{1}{|D|} \sum_{(m_1, m_2) \in D} (I_0(m_1, m_2) - \sum_{t=1}^T \alpha_t I_t(m_1, m_2))^2 \rightarrow \min_{\alpha_1, \dots, \alpha_T} . \quad (2)$$

The last action on this step is calculating both types of errors the mean squared deviation and the normalized mean squared deviation that defined by:

$$\tilde{\varepsilon}_1^2 = \frac{\varepsilon_1^2}{N_1 - 1 \cdot N_2 - 1} \cdot \sum_{i=0}^{N_1-1} \sum_{j=0}^{N_2-1} I_0(i, j)^2 \quad (3)$$

On the  $k = 2^p$  step, every fragment  $I_t(m_1, m_2)$ ,  $t = \overline{1, T}$  corresponding to window  $D$  location is splitted into  $k$  fragments using  $k$ -means clusterization (by brightness) as shown in the Figure 1. New fragments that was constructed after clusterization can be denoted by  $I_t^j(n_1, n_2)$ ,  $j = \overline{0, k-1}$ . Then fragment  $I_0(m_1, m_2)$  is reconstructed by linear combination of fragments  $I_t^j(m_1, m_2)$ :

$$I_0 \approx \sum_{t=1}^T \sum_{j=0}^{k-1} \alpha_t^j I_t^j \quad (4)$$

using mean squared deviation  $\varepsilon_k^2$  minimization:

$$\varepsilon_k^2 \cong \frac{1}{|D|} \sum_{(m_1, m_2) \in D} \left( I_0(m_1, m_2) - \sum_{1 \leq t \leq T} \sum_{0 \leq j \leq k-1} \alpha_t^j I_t^j(m_1, m_2) \right)^2 \rightarrow \min_{\alpha_1^0, \dots, \alpha_1^{k-1}, \dots, \alpha_T^0, \dots, \alpha_T^{k-1}} . \quad (5)$$

Then we calculate both types of errors the mean squared deviation and the normalized mean squared deviation similar to (3):

$$\tilde{\varepsilon}_k^2 = \frac{\varepsilon_k^2}{N_1-1 N_2-1 \sum_{i=0} \sum_{j=0} I_0(i, j)^2}. \quad (6)$$

In the paper, this procedure performs for  $k = 4, 8, 16$ , so there is a set of three mean squared

$$\begin{bmatrix} 3 & 5 & 12 \\ 1 & 14 & 2 \\ 4 & 9 & 17 \end{bmatrix} = \begin{bmatrix} 3 & 5 & 0 \\ 1 & 0 & 2 \\ 4 & 0 & 0 \end{bmatrix} + \begin{bmatrix} 0 & 0 & 0 \\ 0 & 0 & 0 \\ 0 & 9 & 0 \end{bmatrix} + \begin{bmatrix} 0 & 0 & 12 \\ 0 & 14 & 0 \\ 0 & 0 & 0 \end{bmatrix} + \begin{bmatrix} 0 & 0 & 0 \\ 0 & 0 & 0 \\ 0 & 0 & 17 \end{bmatrix}$$

**Figure 1.** Splitting of the fragment  $I_t(m_1, m_2)$  into  $k = 2^2$  fragments.

deviation values and three normalized mean squared deviation values for every position of the window  $D$ . Calculated values presents as  $\bar{x}(n_1, n_2)$  as follows:

$$\bar{x}(n_1, n_2) \equiv \left( \tilde{\varepsilon}_4^2(n_1, n_2), \tilde{\varepsilon}_8^2(n_1, n_2), \tilde{\varepsilon}_{16}^2(n_1, n_2) \right)^T \quad (7)$$

to form the image fragments feature vector. Mean squared deviation values  $\varepsilon_k^2$  are not deliberately taken into account because they are directly used in the calculation of  $\tilde{\varepsilon}_k^2$ .

### 2.2. Statistic construction method

The obtained vectors  $\bar{x}(n_1, n_2)$  set represents in the coordinate system  $\tilde{\varepsilon}_4^2 \tilde{\varepsilon}_8^2 \tilde{\varepsilon}_{16}^2$ . This set locates in the three-dimensional cube with sides equal to 1 as shown in Figure 2:

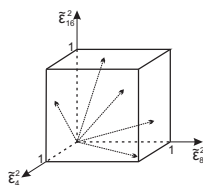


**Figure 2.** The set of feature vectors in the coordinate system  $\tilde{\varepsilon}_4^2 \tilde{\varepsilon}_8^2 \tilde{\varepsilon}_{16}^2$ .

### 2.3. Anomalies determination

There are no absolute static objects on images obtained in real conditions. This is due both to noises of real cameras and the image compression on the path from the camera to the processing system. It often leads to additional system distortions. Moreover, a scene may contain objects that have specific dynamic characteristics although they are static in the global sense. For example, it may be trees swaying in the wind.

As described above, it can be concluded that it is impossible to obtain a feature vector with coordinates  $(0; 0; 0)$  after authentic image fragment representation by described above method. It lets define a rule for assigning fragments corresponding to feature vectors  $(0; 0; 0)$  to anomalies. This type of anomalies refers to fragments that were copied from one or several images of the image time series.

On the other hand, the errors  $\tilde{\varepsilon}_4^2, \tilde{\varepsilon}_8^2, \tilde{\varepsilon}_{16}^2$  of an authentic fragment representation must have values that do not exceed a certain threshold. Feature vectors not corresponded to this condition

are considered anomalies. This type of anomalies refers to fragments that were copied from the same image or image not included in the image time series.

It is obvious the error value of the same fragment representation decreases with the clusters number increasing. Therefore, it is justified to use different thresholds for  $\tilde{\varepsilon}_4^2$ ,  $\tilde{\varepsilon}_8^2$  and  $\tilde{\varepsilon}_{16}^2$ . The following relation should meet:

$$T_{\tilde{\varepsilon}_4^2} \geq T_{\tilde{\varepsilon}_8^2} \geq T_{\tilde{\varepsilon}_{16}^2} \quad (8)$$

Threshold values (8) are defined by analysis the distribution histograms as shown in Figure (3). The first local histogram minimum is selected and considered a threshold value. So, following threshold values were chosen for histograms shown in the Figure 3:

- $T_{\tilde{\varepsilon}_4^2} = 1.5 \times 10^{-8}$ ,
- $T_{\tilde{\varepsilon}_8^2} = 1.5 \times 10^{-8}$ ,
- $T_{\tilde{\varepsilon}_{16}^2} = 0.9 \times 10^{-8}$ .

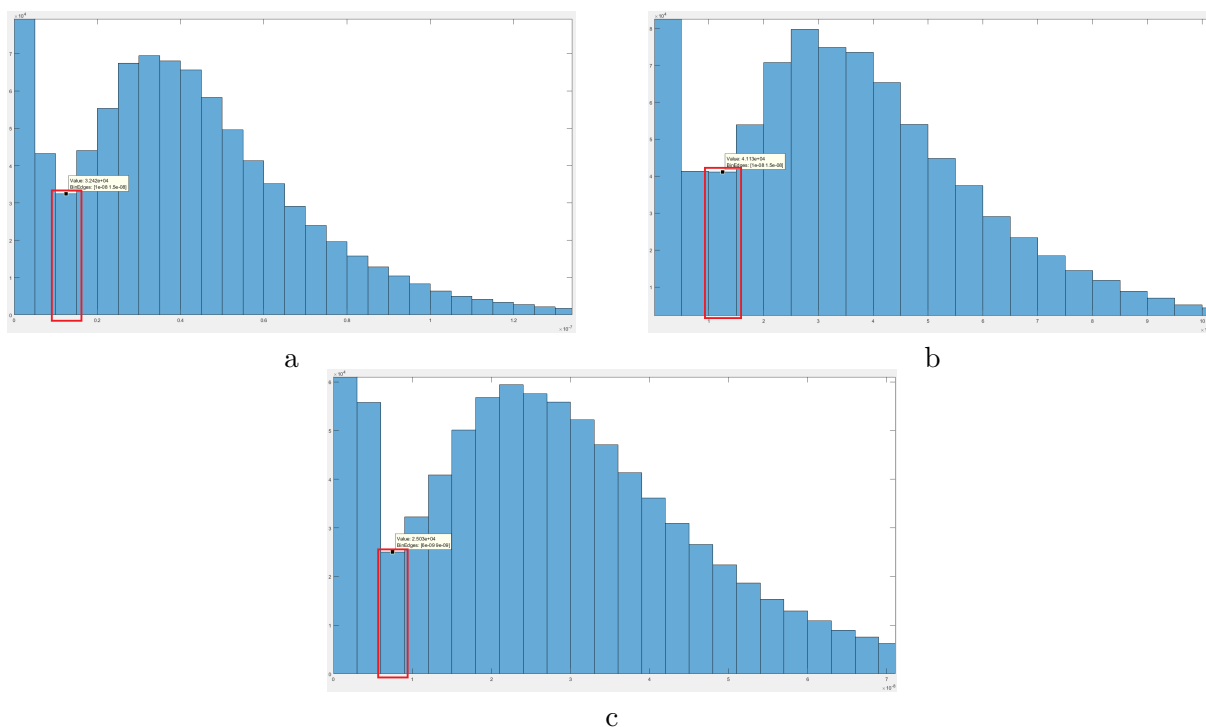


**Figure 3.** Selecting the thresholds according to the distribution histogram: a) for  $\tilde{\varepsilon}_4^2$ , b) for  $\tilde{\varepsilon}_8^2$ , for  $\tilde{\varepsilon}_{16}^2$ .

The cube with the feature vectors  $\bar{x}(n_1, n_2)$  set (2) is divided into three areas:

- 1) Origin of the coordinate system;
- 2) A parallelepiped that is adjacent to the origin;
- 3) Rest area of the cube.

Per the above, feature vectors from the first area correspond to fragments that were copied from one or several images of the image time series. Feature vectors from the second area refer to authentic image regions. Feature vectors from the third area correspond to fragments that were copied within one image or from an image not included in the image time series. This splitting is shown in Figure 4.

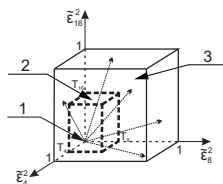


**Figure 4.** Splitting the cube with set of vectors  $\bar{x}(n_1, n_2)$  into three areas.

After extraction of feature vectors from the relevant area and labeling them as suspicious, the corresponded binary mask is created. Then the mask is processed with a noise filter that removes regions with square less than some value. After this, only feature vectors that correspond to forgery regions are kept in the set of suspicious feature vectors.

### 3. Forgery detection using morphological image filtering based on guided contrasting

Morphological image filtering technique based on guided contrasting was proposed in [3]. This filtering technique makes available detecting changing between two images.

An image forgery detection algorithm based on guided contrasting can be performed in two stages:

1. Background normalization based on guided contrasting;
2. Image forgery detection using normalized background image processing.

#### 3.1. Background normalization based on guided contrasting

Let  $f$  - standard image and  $g$  - test image. Proposed in [3] background normalization algorithm gives an opportunity to perform background normalization of the image  $g$  with considering the shape of the image  $f$ . The procedure of background normalization is performed using the window  $D(x, y)$ . The procedure is applied to the pyramid of images with a constant size of the window  $D(x, y)$  to ensure invariance to the window  $D(x, y)$  size.

Background normalization based on guided contrasting is as follows:

1. Construction of the pyramid representation  $f^t = (f^0, \dots, f^{t-1})$  and  $g^t = (g^0, \dots, g^{t-1})$  where  $f^0 = f, g^0 = g$  and  $size(f^i) = \frac{size(f^{i-1})}{2}, size(g^i) = \frac{size(g^{i-1})}{2}, i = \overline{1, t-1}$ .
2. Calculation of the filter (9) response  $\phi^i(f^i, g^i)(x, y)$  for every pyramid level:

$$\phi(f, g)(x, y) = g_0^{D(x,y)}(x, y) + |K(f^{D(x,y)}, g^{D(x,y)})| (g(x, y) - g_0^{D(x,y)}(x, y)), \quad (9)$$

where  $g_0^{D(x,y)}(u, v) = g(x, y), if (u, v) \in D(x, y); 0, otherwise, g_0^{D(x,y)}(x, y) = mean(g^{D(x,y)}(x, y))$  and  $K(f^{D(x,y)}, g^{D(x,y)})$  is the local normalized correlation coefficient defined by (10).

$$K(f, g) = \frac{(f^{D(x,y)} - f_0^{D(x,y)}, g^{D(x,y)} - g_0^{D(x,y)})}{\|f^{D(x,y)} - f_0^{D(x,y)}\| \|g^{D(x,y)} - g_0^{D(x,y)}\|} \quad (10)$$

3. Calculation of absolute difference  $\Delta g_f^i$  between  $g^i$  and corresponding filter response  $\phi^i(f^i, g^i)(x, y)$  for  $i = \overline{1, t-1}$ .

4. Reconstruction of a difference image from the pyramid. It is performed from level  $t-1$  with averaging on every level by following:

$$\Delta m_f^i(x, y) = \{g_f^i(x, y), if i = t-1; max(g_f^i(x, y), h_f^{i+1}(x, y)), otherwise\} \quad (11)$$

where  $h_f^i$  - twofold spatial increased image  $g_f^i$ .

Image  $m_f^0$  is the normalized background of the image  $g$  with considering the shape of the image  $f$ .

### 3.2. Image forgery detection using normalized background image processing

Image  $g$  forgery detection performs by normalized background image  $m_f^0$  processing. This processing carries out as following:

1. Image  $m_f^0$  binarization. For this procedure, thresholding an image with an opportunity to set a threshold by the user was chosen.
2. Morphological filtering of the binary image from step 1 such as erosion and dilation in the square window  $3 \times 3$ .
3. Segmentation and enumeration of all non-zero fragments.
4. Computation of an minimal convex hull of every suspicious segment and fill it.
5. Calculation of the local morphological correlation coefficient (MCC)  $K_M^n$  [4] for every suspicious segment by formula (12) and comparison it with a threshold:

$$K_M^n = \frac{\|g_F^n \chi^n(x, y)\|}{\|g\|} \quad (12)$$

where  $n$  is the number of an analyzed suspicious fragment,  $\chi^n$  is the indicator function that has value "1" for pixels from analyzed suspicious fragment and "0" otherwise and  $g_F^n$  defined by:

$$g_F^n = \frac{(g, \chi^n)}{\|\chi^n\|^2} \quad (13)$$

6. Creating global mask with all forgery fragments which correspond to segments with MCC greater than the threshold.

## 4. Experiments

The experiments were carried out on a desktop PC with Intel Core i5-4460 processor and 16 GB RAM.

Five image time series were obtained using the same camera. The camera was still all the time. It has captured the scene and token image every 10 sec. As result of this procedure, there are five image time series with six images in every series. Obtained images have  $920 \times 1380$  dimension. Next, every image has been transformed to gray-scale. These time series were chosen as the objects of experiments.

Series consisted of six images were used for image forgery detection through the algorithm based on anomaly detection. The algorithm based on guided contrasting used series from two images that are first and last.

Copy-move various type embedding procedure was developed for forgeries generation.

Experiments of two type forgeries detection were carried out:

1. Copy-move within one image - intra-image copy-move.
2. Copy-move from another image of the image time series - inter-image copy-move.

### 4.1. Intra-image copy-move detection

The experiment results with duplicate taken from the same image are shown in the tables 1 and 2. Example of detection using these algorithms is shown in the Figure 5.

As shown in the tables 1 and 2, both algorithms give about the same results of F1 ( 0.66 is mean F1 for the algorithm based on anomalies detection, and 0.59 is mean F1 for the algorithm based on guided contracting). However, these algorithms reach these values on account of different components as so as Precision and Recall. So, the algorithm based on anomalies detection has high values of Recall. It means a greater portion of forgery pixels are detected using the algorithm based on anomaly detection than using the algorithm based on guided

**Table 1.** Intra-image copy-move detection using the algorithm based on anomalies detection.

Series	Precision	Recall	F1
1	0.55	0.84	0.66
2	0.53	0.74	0.62
3	0.62	0.85	0.72
4	0.55	0.68	0.61
5	0.63	0.78	0.70

**Table 2.** Intra-image copy-move detection using the algorithm based on guided contrasting.

Series	Precision	Recall	F1
1	0.93	0.40	0.56
2	0.94	0.67	0.78
3	0.38	0.03	0.06
4	0.50	1	0.68
5	0.86	0.93	0.89

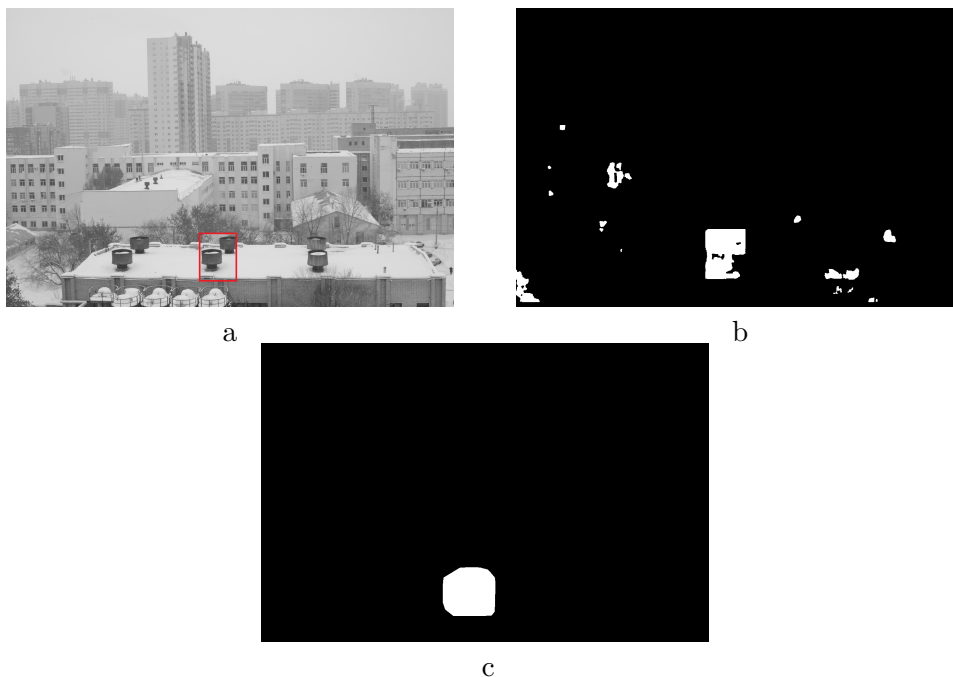


**Figure 5.** Example of intra-image forgery detection: a - forgery image; b - result of detection using the algorithm based on anomalies detection; c - result of detection using the algorithm based on guided contrasting.

contrasting. On another hand, the algorithm based on guided contrasting has high values of Precision. It means this algorithm has less false detection than the algorithm based on anomalies detection.

#### 4.2. Inter-image copy-move detection

The experiment results that were carried out on all image series with duplicate taken from another image of the image series are shown in the tables 3 and 4. Example of detection using these algorithms is shown in the Figure 6.

**Table 3.** Inter-image copy-move detection using algorithm based on anomalies detection.

Series	Precision	Recall	F1
1	1	0.84	0.91
2	1	0.95	0.97
3	0.58	0.74	0.65
4	0.8	0.82	0.8
5	0.87	0.84	0.85

**Table 4.** Inter-image copy-move detection using algorithm based on guided contrasting.

Series	Precision	Recall	F1
1	0.	0.	0.
2	0.75	0.004	0.009
3	0.	0.	0.
4	0.16	0.06	0.09
5	0	0	-

As shown in the tables 3 and 4, the algorithm based on guided contrasting doesn't give opportunity detecting inter-image copy-move forgeries while the algorithm based on anomalies detection does it and give high values of F1.

## 5. Conclusion

The algorithm for image time series forgery detection based on anomaly detection was proposed in this paper. Also, comparison of the proposed algorithm and the algorithm for image forgery detection based on guided contrasting carried out. Experiments showed that both algorithms have about the same quality of detection intra-image copy-move in the sense of metric F1 (0.66 and 0.59 respectively). On another hand, experiments let to conclude that the algorithm of image forgery detection based on guided contrasting doesn't give opportunity detecting inter-image copy-move, unlike proposed algorithm.

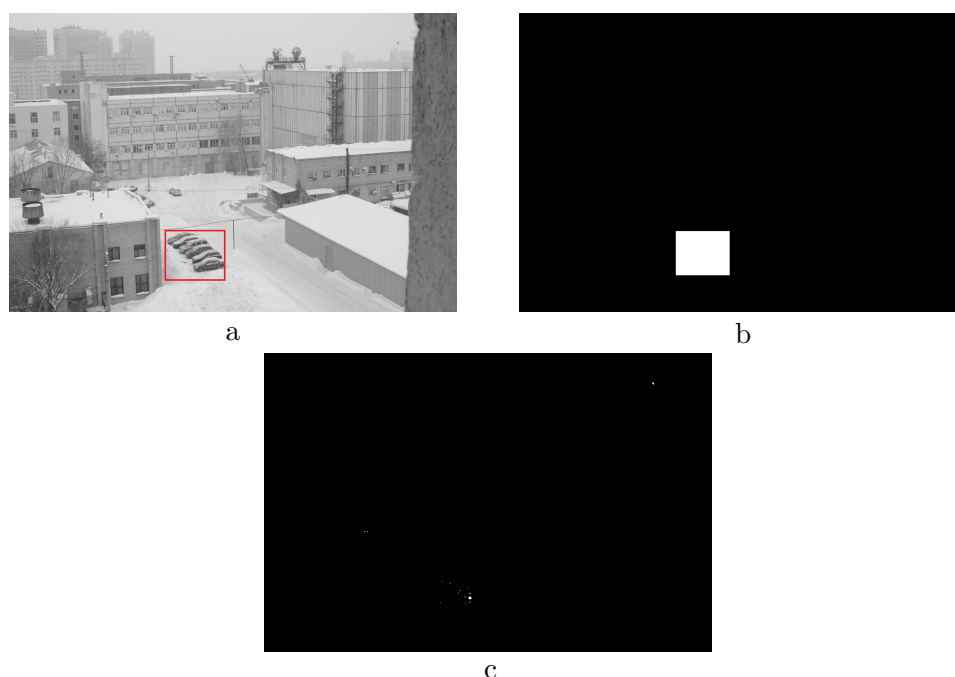


**Figure 6.** Example of inter-image forgery detection: a - forgery image; b - result of detection using the algorithm based on anomalies detection; c - result of detection using the algorithm based on guided contrasting.

## 6. References

- [1] Christian A and Sheth R 2016 Digital video forgery detection and authentication technique - a review *International Journal of Scientific Research in Science and Technology* **2(6)** 138-143
- [2] Chandola V, Banerjee A and Kumar V 2009 Anomaly detection: a survey *ACM Computing Surveys* **41(3)** 51-58
- [3] Rubis A Yu, Lebedev M A, Vizilter Yu V and Vygolov O V 2016 Morphological image filtering based on guided contrasting *Computer Optics* **40(1)** 73-79 DOI: 10.18287/2412-6179-2016-40-1-73-79
- [4] Pyt'ev Yu P and Chulichkov A I 2010 *Methods of Morphological Image Analysis* (Moscow: Fizmatlit)
- [5] Evdokimova N I and Kuznetsov A V 2017 Local patterns in the copy-move detection problem solution *Computer Optics* **41(1)** 79-87 DOI: 10.18287/2412-6179-2017-41-1-79-87
- [6] Kuznetsov A V and Myasnikov V V 2016 A copy-move detection algorithm based on binary gradient contours *Computer Optics* **40(2)** 284-293 DOI: 10.18287/2412-6179-2016-40-2-284-293
- [7] Kuznetsov A V and Myasnikov V V 2014 A fast plain copy-move detection algorithm based on structural pattern and 2D rabin-karp rolling hash *Lecture Notes in Computer Science (including subseries Lecture Notes in Artificial Intelligence and Lecture Notes in Bioinformatics)* **8814** 461-468
- [8] Hussain M, Chen D, Cheng A, Wei H, Stanley D 2013 Change detection from re-motely sensed images: from pixel-based to object-based approaches *ISPRS Journal of Photogrammetry and Remote Sensing* **80** 91-106

## Acknowledgments

The reported study was funded by RFBR according to the research project 17-29-03190, research project 18-01-00748 and by the Federal Agency of scientific organization (Agreement 007-Г3/43363/26).